Performance Analysis of the Access Link of Drone Base Station Networks with LoS/NLoS Transmissions

Huazhou Li[1(✉)], Ming Ding[2], David López-Pérez[3], Azade Fotouhi[4], Zihuai Lin[1], and Mahbub Hassan[4]

[1] University of Sydney, Sydney, Australia
{huazhou.li,zihuai.lin}@sydney.edu.au
[2] Data61, CSIRO, Sydney, Australia
Ming.Ding@data61.csiro.au
[3] Nokia Bell Labs, Dublin, Ireland
david.lopez-perez@nokia.com
[4] University of New South Wales, Sydney, Australia
azade.fotouhi@gmail.com, mahbub.hassan@unsw.edu.au

Abstract. In this paper, we provide performance analysis for drone base station (DBS)-enabled wireless communication networks. The lower bound performance of such networks has been previously obtained in the literature, assuming DBSs are statically hovering and randomly distributed according to a homogeneous Poisson point process (HPPP). We derive the upper bound performance of such networks assuming a teleportation mode, i.e., DBSs can instantaneously move to the positions directly overhead ground users (UEs). By considering both line-of-sight (LoS) and non-line-of-sight (NLoS) transmissions in the access links between DBSs and ground UEs, coverage probability and area spectral efficiency (ASE) are derived in closed-form expressions based on stochastic geometry analysis. The characterization of both the lower and upper bound performances of DBS networks indicates the performance region of practical DBS network operations. Moreover, our analytical and simulation results in this paper provide guidelines for performance optimization of further DBS networks.

Keywords: DBS networks · Performance analysis
LoS/NLoS transmissions

1 Introduction

All but unheard of until just recently, drones – also known as unmanned aerial vehicles (UAVs) – are now envisioned to shape the future of technology [1]. They are among the best candidates to automate emergency search-and-rescue missions, ease crowd management, and act as relays to provide a cellular coverage

T. Q. Duong and N.-S. Vo (Eds.): INISCOM 2018, LNICST 257, pp. 111–121, 2019.
https://doi.org/10.1007/978-3-030-05873-9_10

extension and an ad-hoc capacity boost. A vast growth in the UAV business is also likely to open attractive vertical markets and new revenue opportunities for both mobile network vendors and operators. However, for these technological and commercial visions to turn into a reality, UAVs will require a reliable control and fast wireless connectivity.

Terrestrial cellular networks are well positioned to provide a communication link towards UAVs flying up to an altitude of few hundred meters [2,3]. However, although connecting UAVs through cellular technologies has key potential advantages – such as reusing existing spectrum resources and network infrastructure – it also involves important challenges [4]. Indeed, UAVs may undergo radio propagation characteristics that are profoundly different from those encountered by conventional ground user equipment (UE). UAVs could be placed in locations considerably above ground, experiencing favourable LoS propagation conditions with a vast number of cells. As a result, a UAV transmitting uplink information could create significant interference to a plurality of neighbouring cells receiving ground transmissions. Conversely, cells communicating with their ground UEs could severely disrupt the downlink of a UAV associated to a neighbouring cell [5]. Similar problems arise in operating UAVs as relays, with the addition of energy consumption and autonomy concerns.

With the aim of integrating UAV communications in cellular networks and address those issues, the third generation partnership project (3GPP) has been gathering key industrial players to collaborate on a work item on enhanced cellular support for aerial vehicles [6]. Such ongoing joint effort has already produced systematic measurements and accurate modelling of UAV-to-cell-tower channels, also defining the various UAV link types along with their respective requirements. Simultaneously, the academic community is providing a large number of analytical studies to assess the potential of using UAVs as mobile base stations (BSs). In this context, remarkable progress has been made in optimising the position and trajectory of these flying relays.

Among those, it is worth highlighting the works in [7] and [8]. In the former, the positions of drone base stations (DBSs) were modelled as a three-dimensional Poisson point process (3D-PPP), and a performance analysis was carried for different DBS heights. In the latter, a dynamic re-positioning DBS algorithm was proposed to increase networks spectral efficiency.

In this paper, to characterise the potential gains of DBS networks, we analyse theoretically – using a stochastic geometry analysis (SGA) – the performance upper bound of the DBS to ground UE access link in sparse, dense and ultra-dense networks[1]. In more detail, this performance upper bound is derived, assuming that DBSs can instantaneously move to the positions directly overhead of the ground UEs (teleportation). This study complements that in [9], where a performance lower bound was derived, considering that DBSs were hovering randomly following a homogeneous Poisson point process (HPPP). Importantly, our stochastic geometry model accounts for *(i)* a realistic 3GPP path loss model

[1] Note that the ground BS to DBS backhaul links are considered to be ideal in this paper, and further extensions of this work will study its non-negligible impact.

with both LoS and NLoS transmissions between the DBSs and ground UEs, where a probabilistic function governs the switch between them, and *(ii)* idle modes at the DBSs to switch them off and save energy/mitigate interference when they serve no ground UEs. Using this framework, we derive coverage probability and area spectral efficiency (ASE) expressions, as a function of the DBS and ground UE density. From our analytical and simulation results, the maximum coverage probability and ASE are provided for further investigations on DBS optimization problems.

2 System Model

In this paper, we consider the access link of DBS networks, as shown in Fig. 1. The DBSs are all located at the same height, which is denoted as h_{DBS}. The ground UEs are also all located at the same height, which is denoted as h_{UE}. The absolute antenna height difference between a DBS and a ground UE, i.e., $h_{\mathrm{DBS}} - h_{\mathrm{UE}}$, is denoted by L. In practice, DBSs should not fly too low because of the obvious safety reasons or too high due to the potential performance loss in the backhaul link [9].

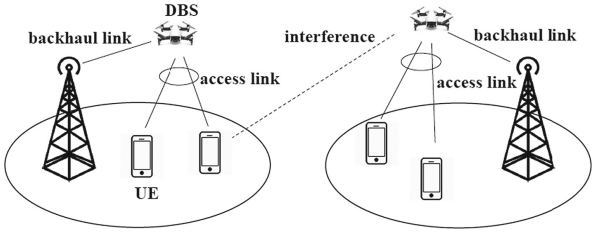

Fig. 1. DBS networks.

The two-dimensional (2D) distance between a DBS and a ground UE is denoted by r. Thus, the 3D distance between a DBS and a ground UE can be expressed as $w = \sqrt{r^2 + L^2}$.

The DBS deployment follows a HPPP distribution with a density λ in an infinite 2D space, while ground UEs are Poisson distributed with a density of λ_{UE} in an infinite 2D space. Note that λ_{UE} may or may not be sufficiently larger than λ, thus there may be DBSs without associated ground UEs in its coverage area.

In practice, a BS will enter an idle mode if there is no UE connected to it, which reduces the interference to UEs in neighbouring cells as well as the energy consumption of the network. As a result, the UE distribution and UE association strategy (UAS) determines the set of active BSs. In this paper, we assume that each ground UE associates with the DBS having the smallest path loss.

Based on the previous considerations and assumptions, the set of active DBSs also follows a HPPP distribution [10], the density of which is denoted by $\tilde{\lambda}$

DBSs/km^2, where $\tilde{\lambda} \leq \lambda$ and $\tilde{\lambda} \leq \lambda_{\mathrm{UE}}$, since one UE is served by at most one DBS. From [10,11], $\tilde{\lambda}$ can be calculated as

$$\tilde{\lambda} = \lambda \left[1 - \frac{1}{(1 + \frac{\lambda_{\mathrm{UE}}}{q\lambda})^q} \right], \tag{1}$$

where according to [11], q also depends on the path loss model.

To derive a performance upper bound of the access link, we can assume that there is always a typical DBS above the head of the typical UE. In this case, we have $r = 0$ and $w = L$. Thus, the DBS and ground UE point processes are identical in the 2D domain, except for height difference of L. This concept is further developed in the next section.

As for the path loss model, in this paper, we use a very general and practical one, in which the path loss $\zeta(w)$ associated with distance w can be segmented into N pieces, and each piece $\zeta_n(w), n \in \{1, 2, \ldots, N\}$ is modelled as

$$\zeta_n(w) = \begin{cases} \zeta_n^{\mathrm{L}}(w) = A_n^{\mathrm{L}} w^{-\alpha_n^{\mathrm{L}}}, & \text{LoS: } \mathrm{Pr}_n^{\mathrm{L}}(w) \\ \zeta_n^{\mathrm{NL}}(w) = A_n^{\mathrm{NL}} w^{-\alpha_n^{\mathrm{NL}}}, & \text{NLoS: } 1 - \mathrm{Pr}_n^{\mathrm{L}}(w) \end{cases}, \tag{2}$$

where $\zeta_n^{\mathrm{L}}(w)$ and $\zeta_n^{\mathrm{NL}}(w), n \in \{1, 2, \ldots, N\}$ are the n-th piece path loss functions for the LoS transmission and the NLoS transmission, respectively, A_n^{L} and A_n^{NL} are the path losses at a reference distance $w = 1$ for the LoS and the NLoS cases, respectively, α_n^{L} and α_n^{NL} are the path loss exponents for the LoS and the NLoS cases, respectively, and $\mathrm{Pr}_n^{\mathrm{L}}(w)$ is the n-th piece LoS probability function that a transmitter and a receiver separated by a distance w has a LoS path, which is assumed to be a monotonically decreasing function with regard to w. In practice, A_n^{L}, A_n^{NL}, α_n^{L} and α_n^{NL} are constants obtainable from field tests.

Moreover, the multi-path fading between a DBS and a UE is modelled as independently identical distributed (i.i.d.) Rayleigh fading in this paper. Results with Rician fading are left for the journal version of this work.

3 Main Results

Using a 3D SGA based on the HPPP theory, we study the performance of a DBS network by considering the performance of a typical UE located at the origin o.

We first investigate the coverage probability, which is defined as the probability that this UE's signal-to-interference-plus-noise ratio (SINR) is above a per-designated threshold γ:

$$p^{\mathrm{cov}}(\lambda, \gamma) = \mathrm{Pr}\left[\mathrm{SINR} > \gamma\right], \tag{3}$$

where the SINR is calculated as

$$\mathrm{SINR} = \frac{P\zeta(w)\, h}{I_{\mathrm{agg}} + N_0}, \tag{4}$$

where h is the channel gain, modelled as an exponential random variable (RV) with the mean of one (Rayleigh fading), P and N_0 are the transmission power of each DBS and the additive white Gaussian noise (AWGN) power at each UE, respectively, and I_{agg} is the cumulative interference given by

$$I_{\text{agg}} = \sum_{i:\, b_i \in \Phi \setminus b_o} P \beta_i g_i, \tag{5}$$

where b_o is the BS serving the typical UE located at distance w from the typical UE, and b_i, β_i and g_i are the i-th interfering BS, the path loss associated with b_i and the multi-path fading channel gain associated with b_i, respectively.

When DBSs are deterministically hovering right on top of the UEs, the access link performance reaches an upper bound, as DBSs are as close to the UEs as they could be. The realisation of such mobile DBSs hovering just above the UEs is difficult, as further considerations on DBSs mobility control management are needed. In this paper, for simplicity, we assume a DBS teleportation model, where DBSs can instantaneously move to the positions just above the UEs, allowing us to derive the upper bound performance of the access links.

Based on the existing expression of $p_{\text{low}}^{\text{cov}}(\lambda, \gamma)$ [12,13], i.e., the lower bound coverage probability, we present our main result on $p_{\text{up}}^{\text{cov}}(\lambda, \gamma)$, i.e., the upper bound coverage probability, in Theorem 1.

Theorem 1.

$$p_{\text{up}}^{\text{cov}}(\lambda, \gamma) = \Pr\left[\frac{P\zeta_n^{\text{L}}(L)\, h}{I_{\text{agg}} + N_0} > \gamma\right], \tag{6}$$

where

$$\Pr\left[\frac{P\zeta_n^{\text{L}}(L)\, h}{I_{\text{agg}} + N_0} > \gamma\right] = \exp\left(-\frac{\gamma N_0}{P\zeta_n^{\text{L}}(L)}\right) \mathscr{L}_{I_{\text{agg}}}^{\text{L}}(s), \tag{7}$$

where $s = \frac{\gamma}{P\zeta_n^{\text{L}}(L)}$, *and* $\mathscr{L}_{I_{\text{agg}}}^{\text{L}}(s)$ *is the Laplace transform of* I_{agg} *for LoS signal transmission evaluated at* s, *which can be further written as*

$$\begin{aligned}\mathscr{L}_{I_{\text{agg}}}^{\text{L}}(s) = \exp&\left(-2\pi\tilde{\lambda}\int_0^{+\infty} \frac{\Pr^{\text{L}}\left(\sqrt{u^2+L^2}\right) u}{1+\left(sP\zeta^{\text{L}}\left(\sqrt{u^2+L^2}\right)\right)^{-1}} du\right) \\ &\times \exp\left(-2\pi\tilde{\lambda}\int_0^{+\infty} \frac{\left[1-\Pr^{\text{L}}\left(\sqrt{u^2+L^2}\right)\right] u}{1+\left(sP\zeta^{\text{NL}}\left(\sqrt{u^2+L^2}\right)\right)^{-1}} du\right),\end{aligned} \tag{8}$$

Proof. As we can see in Theorem 1 of [12], the calculation of the coverage probability is accumulated by components of the coverage probability for the case when the signal comes from the n-th piece LoS path and the n-th piece NLoS path between the typical DBS and the typical UE, respectively.

To derive a performance upper bound of the access links, we can assume that there will always be a DBS located right on top of the typical UE. Under such condition of $r = 0$, i.e., $w = L$, $r_1 = 0$, and $\Pr_1^{\text{L}}(w) = 1$, we can obtain Theorem 1 from Theorem 1 in [12].

According to [12,13], we also investigate the ASE in bps/Hz/km^2, which can be computed as

$$A^{\mathrm{ASE}}(\lambda, \gamma_0) = \tilde{\lambda} \int_{\gamma_0}^{+\infty} \log_2(1+\gamma) f_{\Gamma}(\lambda, \gamma) d\gamma, \tag{9}$$

where γ_0 is the minimum working SINR for the considered DBS, and $f_{\Gamma}(\lambda, \gamma)$ is the probability density function (PDF) of the SINR observed at the typical UE for a particular value of λ.

In the following and to finish this section, we present three concepts that are key to understand the performance behaviour of the studied network, i.e., coverage probability and ASE, which are functions of the DBS density [12–14]. Although originally named after the ASE, these concepts are highly related and apply to the coverage probability explanations too.

- The ASE Crawl
  A much shorter distance between a UE and its serving DBS in ultra-dense networks implies high probabilities of strong LoS transmissions. Generally speaking, LoS transmissions are helpful to improve the signal power, but they aggravate the interference too. Thus, the ASE will suffer from a slow growth or even a decrease when the DBS density is sufficiently large, and the stronger interference paths transition from NLoS to LoS. This performance behaviour is referred to as the ASE Crawl [12].
- The ASE Crach
  The existence of a non-zero antenna height difference between UEs and DBSs leads to a non-zero cap on the minimum distance between them, and thus a cap on the signal power strength. Although each inter-cell interference power strength is subject to the same cap, the aggregated inter-cell interference power will overwhelm the signal power in an ultra-dense network due to the sheer number of strong interferers. Thus, the ASE will suffer from a significant loss when the DBS density is sufficiently large. This performance behaviour is referred to as the ASE Crash [14].
- The ASE Take-off
  When the number of DBSs is larger than that of UEs, the surplus of DBSs encourages idle mode operations to mitigate unnecessary inter-cell interference and reduce energy consumption. Consequently, the SINR performance benefits from *(i)* a DBS diversity gain in UEs selecting a good serving DBS, and *(ii)* a decreased inter-cell interference, which is bounded by the active UE density. As a result, the signal power continues increasing with the network densification, while the interference power reduces or remains at a constant level due to the idle mode capability. This performance behaviour is referred to as the ASE Take-off [13].

4 Simulation Results

In this section, we use simulation results to verify the accuracy of our analysis. It is important to note that there are no specific system model recommendations available for a DBS network. Fortunately, however, models for the channel

between the terrestrial BSs and the ground UEs are provided for different scenarios [15], which can be reused in our simulation, treating terrestrial BSs as DBSs. Specifically, and according to 3GPP [15], we reuse the urban macro (UMa) and the urban micro (UMi) terrestrial BS channel models, adopting the parameters shown in Table 1.

Table 1. Parameters.

	UMa model	UMi model
h_{DBS}	25 m	10 m
α_n^{L}	2.2	2.1
α_n^{NL}	3.908	3.53
A_n^{L}	$10^{-2.8-2\log_{10} f_c}$	$10^{-3.24-2\log_{10} f_c}$
A_n^{NL}	$10^{-1.354-2\log_{10} f_c}$	$10^{-2.24-2.13\log_{10} f_c}$
P	46 dBm	41 dBm
h_{UE}	1.5 m	1.5 m

Moreover, we adopt the following parameter values: $N_0 = -95\,\mathrm{dBm}$, $q = 3.5$, $\lambda_{\mathrm{UE}} = 300\,\mathrm{UEs/km}^2$, $\gamma = 0\,\mathrm{dB}$ and $f_c = 2\,\mathrm{GHz}$. The LoS probability function for both models is given by [15] and shown as below:

$$\Pr^{\mathrm{L}}\left(\sqrt{r^2+L^2}\right) = \begin{cases} 100\%, & r \le 18\,\mathrm{m} \\ (18/r + \exp(-r/63) * (1 - 18/r)), & r > 18\,\mathrm{m} \end{cases}, \tag{10}$$

where r is the 2D distance, and $L = h_{\mathrm{DBS}} - h_{\mathrm{UE}}$. Note that $\Pr^{\mathrm{L}}\left(\sqrt{r^2+L^2}\right) = 1$ in the teleportation mode, since $r = 0$.

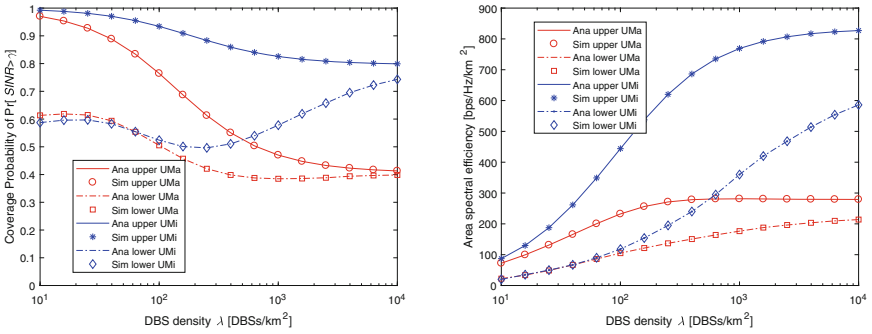

(a) Coverage Probability vs. λ with γ=0dB. (b) ASE vs. λ with γ=0dB.

Fig. 2. Networks performance

4.1 Coverage Probability Analysis

As can be seen from Fig. 2a, we analyse $p_{\text{up}}^{\text{cov}}(\lambda, \gamma)$ and $p_{\text{low}}^{\text{cov}}(\lambda, \gamma)$ for the UMa and UMi models, respectively. It is important to note that the result of $p_{\text{up}}^{\text{cov}}(\lambda, \gamma)$, given by Theorem 1, perfectly match the simulation results, which validates the accuracy of our analysis.

Coverage Probability of the UMa Model

- Upper bound performance
  - At low DBS densities, the probability of coverage, $p_{\text{up}}^{\text{cov}}(\lambda, \gamma)$, is high, around 97%. This is due to the high signal power, provided by the DBS overhead the typical UE, and the low interference power, common in sparse networks. The majority of interference links are NLoS ones.
  - As λ increases, the distances between DBSs become smaller and thus the inter-cell interference increases, and as a result, $p_{\text{up}}^{\text{cov}}(\lambda, \gamma)$ monotonically decreases. The major decrease happens when $\lambda \approx 100\,\text{DBSs/km}^2$. This is due to the ASE Crawl [12], i.e., a large number of interference transit from NLoS to LoS.
  - When $\lambda > \lambda_{\text{UE}}$, $p_{\text{up}}^{\text{cov}}(\lambda, \gamma)$ decreases at a much slower rate due to the combined effect of the ASE Crash and the ASE Take-off [13,14], with the former effect being stronger. Although the antenna height difference will lead to the severe loss of coverage probability in the ultra-dense network, the idle mode at BSs effectively mitigates the inter-cell interference.
- Lower bound performance
  - The result of $p_{\text{low}}^{\text{cov}}(\lambda, \gamma)$ is obtained from [14], where it was assumed that the DBSs are randomly deployed.
  - When λ is around $30\,\text{DBSs/km}^2$, $p_{\text{low}}^{\text{cov}}(\lambda, \gamma)$ moderately increases due to the enhancement of LoS signal power.
  - When $\lambda \in [30, 300]\,\text{DBSs/km}^2$, $p_{\text{low}}^{\text{cov}}(\lambda, \gamma)$ suffers from a significant loss, from around 60% to less than 40%. Similar as that for the upper bound, this is due to the ASE Crawl.
  - When $\lambda > \lambda_{\text{UE}}$, $p_{\text{low}}^{\text{cov}}(\lambda, \gamma)$ slowly recovers to 40%. Similar as that for the upper bound, this is also caused by the combined effect of the ASE Crash and the ASE Take-off.
  - The lower bound performance of the coverage probability converges to the upper bound one in the ultra-dense networks, as there is always a DBS very close to each ground UE.

Coverage Probability of the UMi Model

- Upper bound performance
  - We can see from Fig. 2a that the the upper bound performances trend of the UMi model is similar to that of the UMa one. However, it is important to note that $p_{\text{up}}^{\text{cov}}(\lambda, \gamma)$ of the UMi model is always better than that of the UMa one, since a lower antenna height provides a stronger signal power and postpones the ASE Crash [14].

- Lower bound performance
  - The lower bound performance trend of the UMi model is also similar to the UMa one. Due to the enhancement of LoS signal link, $p_{\text{low}}^{\text{cov}}(\lambda, \gamma)$ also slowly increases when $\lambda \in [10, 30]$DBSs/km^2. Then, $p_{\text{low}}^{\text{cov}}(\lambda, \gamma)$ first decreases due to the ASE Crawl and ASE Crash, and then increases due to the ASE Take-off. The last increase is more significant as the ASE Crash effect is weaker due to the lower antenna height in the UMi model. Moreover, note that $p_{\text{low}}^{\text{cov}}(\lambda, \gamma)$ of the UMi model is less than $p_{\text{low}}^{\text{cov}}(\lambda, \gamma)$ of the UMa one until $\lambda > 40$ DBSs/km^2. After that, it is the other way around. This is due to lower transmission power and different LoS probability functions, as shown in Table 1.

4.2 Area Spectral Efficiency Analysis

In Fig. 2b, we present the results of the ASE performance for both the UMa and UMi model, respectively. As we can see from Fig. 2b, the analytical results and simulation results are perfectly matched.

ASE of the UMa Model

- Upper bound performance
  - It can be seen from Fig. 2b that the ASE is about 80 bps/Hz/km^2 when the network is sparse, and the ASE keeps increasing to the maximum value near 300 bps/Hz/km^2 when λ is about 300 DBSs/km^2 due to the larger spectrum spatial reuse.
  - The ASE upper bound decreases its growth rate when $\lambda > 300$ DBSs/km^2 due to the degraded coverage probability as a result of the combined effect of the ASE Crash and the ASE Take-off.
- Lower bound performance
  - The ASE is around 10 bps/Hz/km^2 when the network is sparse, and then it keeps monotonically increasing with the DBS density, reaching around 200 bps/Hz/km^2 when λ is around 10^4 DBSs/km^2. There is no decrease as in the upper bound, because the coverage probability remains almost constant with the BS density in this case, and the spatial reuse dominates the ASE performance. The gap to the upper bound performance in this ultra-dense network is about 90 bps/Hz/km^2.

ASE of the UMi Model

- Upper bound performance
  - As shown in Fig. 2b, the upper bound performance of ASE for the UMi model is always better than that of the UMa model due to the superior performance of coverage probability, as shown in Fig. 2a.
  - Note that compared with the results for the UMa model, the upper bound performance of ASE for the UMi model grows faster for all DBS densities. This is due to the smaller antenna height difference, which leads to the stronger signal power and postpones the ASE Crash.

- Lower bound performance
  - The lower bound performance of ASE for the UMi model shows a similar trend compared with that for the UMa model when $\lambda < 100\,\text{DBSs/km}^2$. But after that, it exceeds the UMa lower bound, which is also caused by different coverage probability performance of the two models.

5 Conclusion

In this paper, we derive an upper bound for the performance of DBS networks, by assuming DBSs can move instantaneously over the serving UEs' head (teleportation mode). Both coverage probability and ASE are derived using a practical channel model adopted by the 3GPP. Numerical results characterize the theoretical performance limit that can be achieved by future DBS networks, with various DBS densities, heights and DBS trajectory optimizations.

References

1. New America: Drones and aerial observation: new technologies for property rights, human rights, and global development - a primer, July 2015
2. Mozaffari, M., Saad, W., Bennis, M., Debbah, M.: Communications and control for wireless drone-based antenna array. arXiv:1712.10291, December 2017
3. Lyu, J., Rui Zhang, Y.Z.: UAV-aided offloading for cellular hotspot. IEEE Trans. Wirel. Commun. **17**, 3988–4001 (2018)
4. Geraci, G., Garcia Rodriguez, A., Giordano, L.G., López-Pérez, D., Björnson, E.: Understanding UAV cellular communications: from existing networks to massive MIMO. arXiv:1804.08489, April 2018
5. Geraci, G., Garcia Rodriguez, A., Giordano, L.G., López-Pérez, D., Björnson, E.: Supporting UAV cellular communications through massive MIMO. In: Proceedings of the IEEE ICC Workshops, May 2018. arXiv:1802.01527 (2018, to appear)
6. 3GPP Technical Report 36.777: Technical specification group radio access network; Study on enhanced LTE support for aerial vehicles (Release 15), December 2017
7. Zhang, C., Zhang, W.: Spectrum sharing for drone networks. IEEE J. Sel. Areas Commun. **35**(1), 136–144 (2017)
8. Fotouhi, A., Ding, M., Hassan, M.: Dynamic base station repositioning to improve spectral efficiency of drone small cells. In: IEEE 18th International Symposium on A World of Wireless. Mobile and Multimedia Networks (WoWMoM), pp. 1–9 (2017)
9. Ding, M., López-Pérez., D.: Please lower small cell antenna heights in 5G. In: IEEE Global Communications Conference (GLOBECOM), pp. 1–6 (2016)
10. Mozaffari, M., Saad, W., Bennis, M., Debbah, M.: Drone small cells in the clouds: design, deployment and performance analysis. In: 2015 IEEE Global Communications Conference (GLOBECOM), pp. 1–6 (2015)
11. Madhusudhanan, P., Restrepo, J.G., Liu, Y., Brown, T.X., Baker, K.R.: Downlink performance analysis for a generalized Shotgun cellular system. IEEE Trans. Wireless Commun. **13**(12), 6684–6696 (2014)
12. Ding, M., Wang, P., López-Pérez, D., Mao, G., Lin, Z.: Performance impact of LoS and NLoS transmissions in dense cellular networks. IEEE Trans. Wirel. Commun. **15**(3), 2365–2380 (2016)

13. Ding, M., López-Pérez, D., Mao, G., Lin, Z.: Performance impact of idle mode capability on dense small cell networks. IEEE Trans. Veh. Technol. **66**(11), 10446–10460 (2017)
14. Ding, M., López-Pérez, D.: Performance impact of base station antenna heights in dense cellular networks. IEEE Trans. Wirel. Commun. **16**(12), 8147–8161 (2017)
15. 3GPP: TR 38.901(v14.0.0) Study on channel model for frequencies from 0.5 to 100 GHz (2017)